

# Automatic Detection of White Blood Cancer from Bone Marrow Microscopic Images Using Convolutional Neural Networks

SK.JABEENA<sup>1</sup>, SK.NAZMA SULTHANA<sup>2</sup>,  
ASSISTANT PROFESSOR<sup>1,2</sup>,  
DEPARTMENT OF ECE

PBR VISVODAYA INSTITUTE OF TECHNOLOGY AND SCIENCE::KAVALI

## ABSTRACT

*The bone marrow is responsible for producing about 1% of all blood cells, which are known as leukocytes. Blood malignancy originates in the unchecked multiplication of these neutrophils. The suggested research offers a reliable method for categorizing three distinct kinds of cancer. Multiple Myeloma (MM) and Acute Lymphoblastic Leukemia (ALL) use the SN-AM dataset. In cases of acute lymphoblastic leukemia (ALL), an abnormally high number of lymphocytes are produced by the bone marrow. However, unlike other cancers, multiple myeloma (MM) causes malignant cells to collect in the bone marrow rather than being disseminated throughout the body. As a result, they inhibit the development of new, healthy blood cells by crowding them out. In the past, this would take a very long time and a lot of effort on the part of a trained expert. Using deep learning methods, specifically convolutional neural networks, the suggested model eliminates the possibility of mistakes in the human process. The algorithm is educated on pictures of cells, so it knows how to best pre-process and retrieve characteristics from those images. Next, the sort of malignancy in the cells is predicted by training the model using an improved version of the Dense Convolutional neural network (DCNN) architecture. While remembering the samples precisely 94 times out of 100, the model accurately reproduced all the data.*

## I. INTRODUCTION

CELLS Red blood cells, platelets, and white blood cells are the three kinds of blood cells. They are all produced in the bone marrow and secreted constantly. Prompt in the circulatory system. The primary reason why people get blood cancer is because aberrant blood cells multiply at an exponential rate, stunting the development of healthy blood cells. Leukemia, myeloma, and lymphoma are the three most common forms of blood malignancy. Acute lymphocytic leukemia is a malignancy of white blood cells that primarily affects the bone marrow. (ALL). The term "acute" is used to describe diseases that advance rapidly and, if left untreated, Can be deadly in a relatively brief amount of time [1, 2]. Each type of ALL is designated as L1, L2, or L3 [3]. Multiple myeloma (MM) is trachoma of embryonic plasma cells that aid in the removal of infection [4]. The frequency is three times that of ALL. In contrast to leukemia, the patient with this condition has a normal white blood cell count but a reduced red blood cell count because harmful cells are taking up room that would otherwise go to RBCs. Thrombocytopenia, or a decreased number of platelets in the circulation, is caused by multiple myeloma. [5] Erosion is another effect. Identified via CT images as bone tumors. [6] In 2019, this illness will be responsible for the fatalities of about 1500 individuals, or about 0.2% of all cancer-related deaths [7]. Every year in the United States, nearly 20,000 individuals are identified with myeloma. Blood cancer treatment varies by patient age, cancer type, cancer stage, contaminated regions, and other factors [8]. One of the primary elements in determining the classification of blood cancer is the blood level. Manual and automated numbering methods are both possible. Manual processing takes longer but yields a perfect identification rate in the hands of an expert [9]. Automatic numbering, on the other hand, saves time but increases the likelihood of an inaccurate tally. It follows that there are benefits and drawbacks to both approaches. This article provides a high-level summary of the automated method for classifying white-blood-cell malignancies. Automatic categorization saves time and money and can be implemented rapidly in both metropolitan and country regions. Inconsistencies resulting from human categorization labor, the need for an expert, and other issues are introduced by the suggested system. The blunders brought on by the fact that cells look the same under a microscope, etc. All of these problems can be solved with the

aid of deep learning-based methods [10], as these techniques extract useful characteristics from the original data. When dealing with a big number of pictures, Deep Learning has been shown to perform better than traditional Machine Learning [11]. With just a little bit of preparation, the outcomes of Convolution Neural Networks (CNNs) that blend multiple layered perceptions are impressive. [12] CNNs acquire a new feature that is present in the pictures and thus generates a high activation, making the CNN itself a feature generator. The suggested research uses Convolution Neural Networks to offer a powerful and reliable automatic categorization technique for identifying the sort of white blood malignancy, specifically Acute Lymphoblastic Leukemia (ALL) and Multiple Myeloma (MM). Therefore, the paper compares the suggested deep learning model's performance against a set of benchmarks, including accuracy, precision, memory, sensitivity, and specificity. What this piece really adds to the discussion is: To identify cancer types from a limited dataset, the suggested model adopts a generic strategy. Data enhancement has been used for extension. On the recovered and prepped dataset, the suggested DCNN has been shown to outperform some state-of-the-art CNN models through comparison analysis. The suggested model beats state-of-the-art machine learning and pre-trained deep learning models in classifying cancer types despite requiring less processing time and having trainable parameters.

This report followed the following outline: The associated study is discussed in Section II. The suggested method for blood cancer classification, learning metrics, a summary of the dataset, and the evaluation approach are described in Section III. In Section IV, we present the findings of our extensive trials with the suggested model and draw comparisons to more conventional machine learning methods.

## II. RELATED WORK

The study of pictures of infectious blood cells usually consists of three phases: image preparation; feature extraction; feature selection; and categorization. A lot of work has been put into investigation into numerous forms of malignancy (particularly leukemia, lymphoma, and myeloma). In order to directly classify cervical cells into infectious and normal cells without segmenting them, Zhang et al. [13] suggested a convolutional neural network model. In order to categorize the different WBCs found in the body, Zhao et al. [12] suggested the use of machine learning methods such as CNN, SVM, Random Forests, etc. Instead of training the images in RGB space, the suggested Stain Deconvolution Layer (SD Layer) for identifying cancerous and healthy cells instead learned from the images in the Optical Density (OD) space [14].

FORAN et al. created a prototype for a clinical decision support system that uses picture processing to distinguish between different types of blood tumors and is then given to the patient. The algorithm provided picture analysis using the "gold standard" dataset and therapy recommendations using the number reasoning of the accumulated instances [15]. The article demonstrates a method for picture categorization using a convolutional neural network (CNN) [16] by first improving, then expanding, and lastly handling the training data. The results are then applied to photos of Human Epithelial Type 2 cell IIF. Before using the ALL-IDB dataset for AML classification, it is first modified in various ways, including histogram normalization, reflection, translation, and rotation. Distortion, fuzziness, etc. Seven layers of convolutional neural networks are used in the end [17]. To identify Acute Lymphocytic Leukemia (ALL) from tiny blood sample pictures, Shrutika Mahajan et al. [18] suggested an SVM-based system with modifications to texture, shape, and histogram as the classifier's inputs. One of the articles considered an illustration of an extraction aircraft in green. The authors suggested using a completely linked network to classify breast cancer pictures after feature extraction via CNN.

## III. PROPOSED METHODOLOGY

The model is learned on the training set, and then it is used to make predictions on the test set. The model consists of three different layers: a convolution layer, a max pool layer, and a completely linked layer. Control group. Figure 1 depicts the process flow of the suggested approach.

### A. DATASET DESCRIPTION

The sample for the suggested research is drawn from two distinct parts of a larger compilation [29]. The collection begins with pictures of people who have B-ALL. Specifically, there are 90 pictures of B-Lineage Acute Lymphoblastic Leukemia. The ALL image's backdrop mask and nucleus mask are displayed in Figure 2. The other 100 pictures come from individuals who have been identified with multiple myeloma and make up the second portion of the collection.

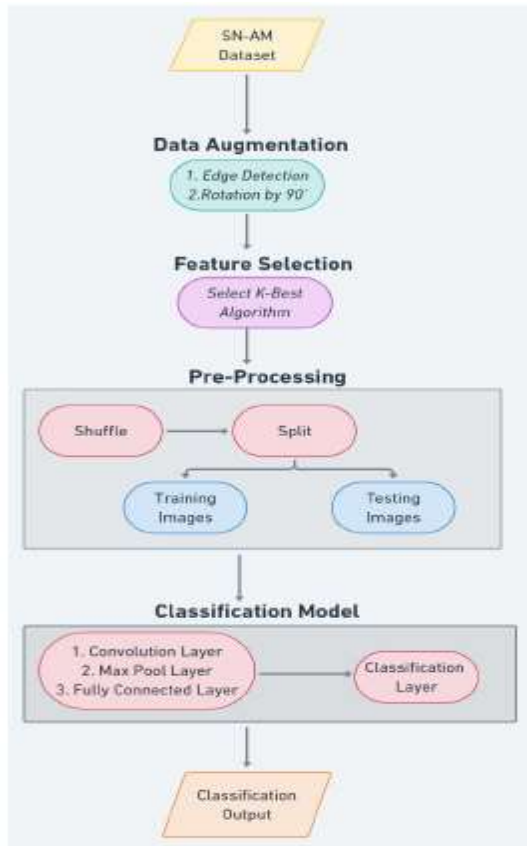


FIGURE 1: Proposed Methodology.

The masks for the backdrop, nuclei, and cytoplasm of plasma cells for the matching MM picture are displayed in Figure 3. 2560 x 1920 resolution images please. The collection is comprised of images in BMP format. The suggested CNN model for classifying cancer cells as either ALL or MM is trained using the mixed version.

## B. DATA AUGMENTATION

Before adding it to the SN-AM collection, we rotate the picture and remove the borders. The jumbled pictures are then split up into an instruction set and an exam group. There needs to be a major for the model to apply well during testing, there needs to be a large quantity of data accessible, with the target item present in a variety of sizes, positions, and illumination conditions. Using different picture manipulation methods, data can be synthesized from preexisting data. Photo 4.

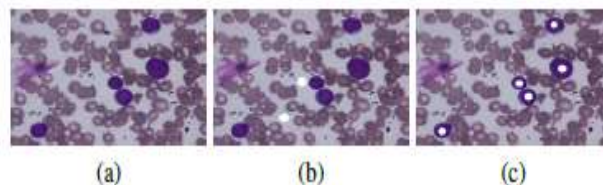
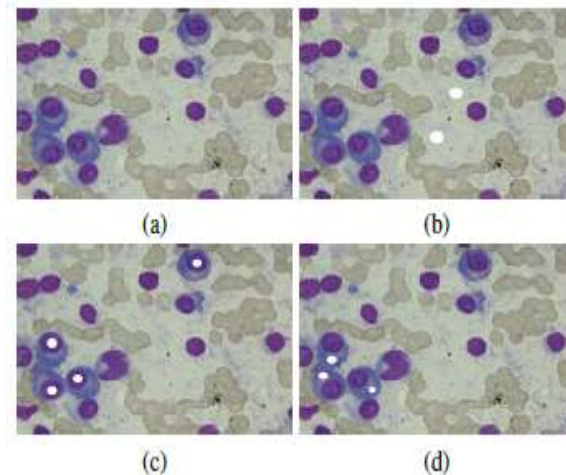


FIGURE 2: Images from the FULL Dataset as examples. Sample picture (a), backdrop mask (b), and nucleus mask (c) in their entirety. Acute lymphoblastic leukemia is abbreviated as "ALL."

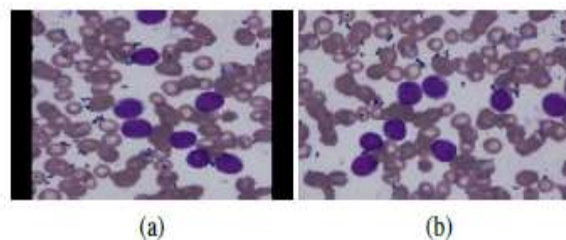


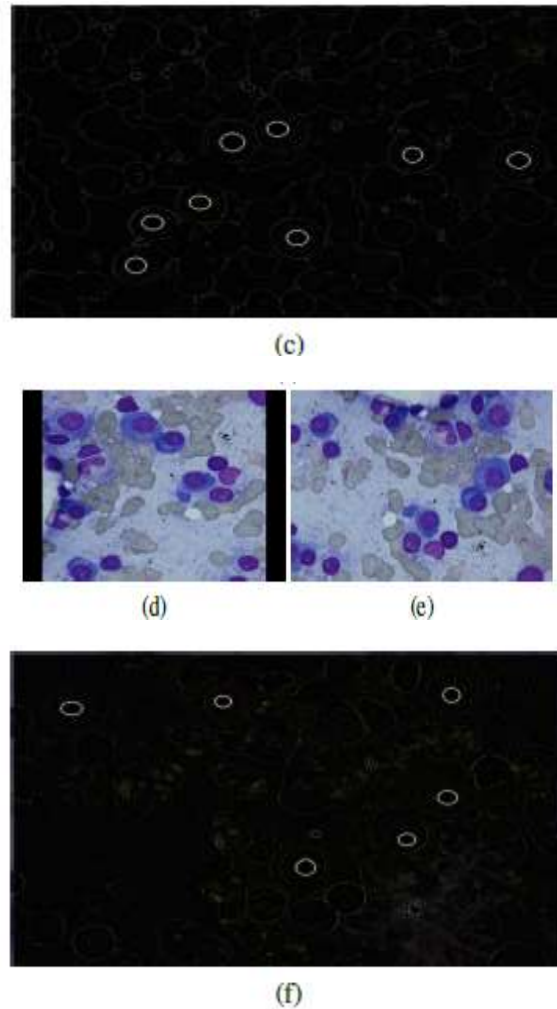
Pictures taken from the MM Dataset (Figure 3). Masks for the nucleus (c) and cytoplasm (d) of an MM sample picture (a). The letters MM denote the diagnosis of multiple myeloma. Displays the final pictures after data enhancement has been applied. The first method is a simple 90-degree shift of the pictures [30]. To ensure that our model can identify the object in any direction, we spin all the pictures by 90 degrees, as shown in Figures 4(b) and 4(c).(e). Figures 4(c) and 4(d) depict the next method, which screens the image and gives a filtered version of the image consisting only of the borders or limits of the original image. (f). Over fitting occurs without data supplementation, making it hard for the model to apply to new instances that were not included in the training set.

### C. FEATURE SELECTION

In Deep Learning, Feature Selection is critically important and has a huge impact on model success. When a model has too many characteristics, its accuracy suffers. Feature Selection is the process of deciding which characteristics to use in order to influence the outcome. Reduced over-fitting because less duplicate data removes the possibility of forecasts based on noise is one of the main benefits of this method. Having less material to learn on means less effort spent in training, as the erroneous information and anomalies are filtered out, precision increases. Univariate feature selection was used in the suggested research. With univariate feature selection, you look at each feature independently to determine how strongly it correlates with the dependent variable.

The Select Best utilizes a battery of statistical evaluations





Micrographs with added data (Figure 4).

A UNIQUE ORIGINAL IMAGE (a). (B) The entire initial picture has been turned counterclockwise by 90 degrees. (c) Identified Marginal Areas in the Original ALL picture, (d) the initial MM picture. (e) The initial MM photo turned counterclockwise by 90 degrees. (f) The MM image's detected edges. K-specific characteristics can be chosen based on the patient's cancer class (ALL denotes acute lymphoblastic leukemia; MM denotes multiple myeloma). The Chi-square ( $\chi^2$ ) test is utilized in the suggested model. The chi-square test is used to determine whether or not two occurrences are independent in the realm of statistics. Given information about two factors, we can derive an "observed count" of O and a "predicted count" of E. Chi-square analyses the discordance between the expected (E) and actual (O) numbers. We pick characteristics with an eye toward maximizing their dependence on the outcome variable. When the two characteristics are separate, the measured count is near to the anticipated count, giving us a lower Chi-square number. Therefore, the large Chi-square number disproves the independence theory. Therefore, if the Chi-square value is high, the feature is highly response-dependent and should be chosen for model training. Select Best, in its simplest form, computes scores for each feature and then discards all but the K highest-scoring features.

The solution for the chi-squared test is shown in Equation (1).

$$\chi^2 = \frac{(O - E)^2}{E} \quad (1)$$

If there were no correlation between the characteristic and the result, then the anticipated number of class observations would be  $E$ , where  $O$  is the total number of class observations.

#### D. PRE-PROCESSING OF IMAGES

Data pre-processing entails a wide range of operations, such as dealing with missing values, one-hot encoding, normalization, multi-co linearity, scaling, randomization, and division. The suggested research will involve after feature selection and transformation, the resulting data is first standardized before being randomly split into training and testing groups. The sample is split 75/25 in favor of model training and testing.

#### E. PROPOSED CONVOLUTION NEURAL NETWORK AND ARCHITECTURE

In this research, we propose a new CNN method to enhance this process. The cancer type has been identified; it is either ALL or MM. This is used in the training of our deep learning model. It's illustrated in Figure 5. CNNs, or Convolutional Neural Networks, are a type of neural network. Mainly used for research involving visual media. The important role that CNNs play in picture classification algorithms. When it comes to picture classification, the crew works quickly and accurately. They use relatively little preparation when compared to other picture classification techniques. A standard CNN model has an input layer, a hidden layer, a layer in the middle, and an output layer. An unprocessed image is given to the proposed algorithm in this paper, and a cancer categorization is anticipated to be returned. (Either ALL or MM). The paper's main CNN design is presented in Table 1. Layer 1 Convolution First, the picture data is fed into the convolution layer. Synapses are the fundamental units from which individual traits are derived. A causative map is produced when a filter (kernel matrix) is applied to a raw picture the number of steps by which the filter moves across the image, as decided beforehand. Applying convolution to a raw image of size  $a \times b$  pixels centered on a core of size  $k$  plus Extra padding,  $p$  in a single bound, Amount as output

$$(a - k + 2p) / s + 1 \times (b - k + 2p) / s + 1.$$

Furthermore, different training pictures will result in different filtering granularities. Two convolution layers with softmax activation are present in the suggested model. Routines and then a sharing layer. Equation gives the usual definition of the softmax function  $\sigma: \mathbb{R}^K \rightarrow \mathbb{R}^K$ . (2). Convolution of the input picture with the kernel function yields the activation map, which is given by Eq. (3).

$$\sigma(\mathbf{z})_i = \frac{e^{z_i}}{\sum_{j=1}^K e^{z_j}} \quad (2)$$

$$A[x, y] = (I * f)[x, y] = \sum_i \sum_j I[i, j] f[x - i, y - i] \quad (3)$$

where  $I$  is the input picture,  $f$  is the kernel function,  $x$  and  $y$  are the row and column counts of the output matrix,  $i$  and  $j$  are the row and column counts of the input matrix, and the picture data array in each case.

#### 2) Pooling Layer

The pooling layer, which functions as a non-linear down-sampling layer, is another central idea in CNNs. In this approach, the non-linear max-pooling function is used to allocate resources. Divides the picture into non-overlapping areas and then returns the highest number for each of those parts. The main goal of the pooling layer is to limit over fitting by reducing the number of parameters and the quantity of processing required by the network. Using a kernel of size  $k$  and a step size  $s$ , max-pooling takes a picture of size  $a \times b$  and finds the highest value within a defined area.  $(ak) = (s+1) \times (Bk) = (s+1)$  is the quantity of the result that this process generates. Figure 6 shows how a picture is down sampled by a max-pooling layer.

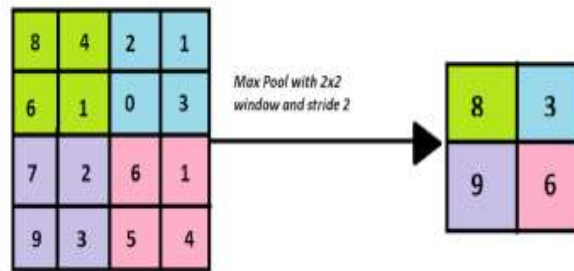


FIGURE 6: Maxpool Function

### 3) Fully Connected Layer

Multi-Layer Perceptions have completely linked layers. After a series of convolution layers, a thick layer is applied. A completely linked layer, as the term implies, establishes a connection between every cell in two or more layers. They use the characteristics gleaned from the convolutions in the same way that conventional neural networks do: to categorize pictures. The mistake is computed and back-propagated at this stage. The suggested model has five interconnected levels, the fifth of which is the output layer. All four completely linked levels use the softmax triggering algorithm. The sigmoid activation function is present in the output layer, and it generates a chance between 0 and 1 for each of the categorization categories that the model is attempting to forecast. This equation gives the definition of the sigmoid function. (4).

$$Sig(z) = \frac{1}{1 + e^{-z}} = \frac{e^z}{e^z + 1} \quad (4)$$

Here,  $z$  is the input vector.

TABLE 1: Network Architecture.

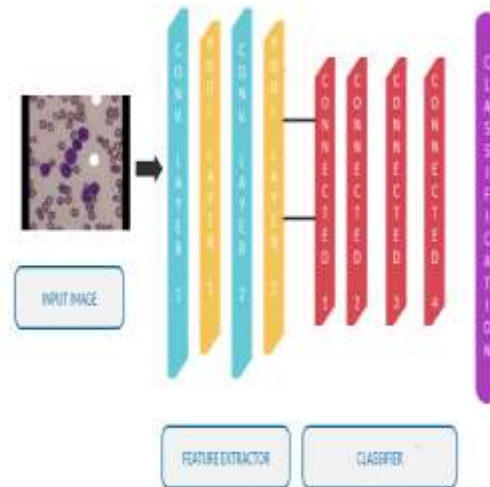


FIGURE 5: A Suggested Framework for a CNN Model.

Pseudo-code for the deep learning-based picture classification method is presented in method 1.

## IV. RESULTS AND ANALYSIS

The categorization algorithm is developed on the end-to-end open-source framework Tensor Flow. Over the course of 1000 trials, a binary categorization model was learned using 424 pictures. After each cycle, achieves a minimal loss at the final run by optimizing the loss function with the Adam Optimizer. The learned algorithm was then used to make inferences about the cancer subtypes depicted in the pictures. In order to develop the model, a K80 GPU is used. First, the outcomes of the suggested paradigm will be described. The suggested model is compared to the state-of-the-art in machine learning and deep learning, and the results of these comparisons are discussed.

## A. DEEP LEARNING APPROACH

With a learning rate of 0.01 and an algorithm for changing weights, we use Adam Optimizer to train our network in the CNN portion. (5). the sigmoid loss function is implemented. The Adam algorithm finds the best value for the cross-entropy loss function. As shown in Figure 8, damage decreases as the repetition count rises. After 800 training rounds, the training loss stabilizes at a fixed number, as depicted in the figure. After 1000 rounds, we get to the lowest number, which is 0.5034. The confusion matrix for CNN-based binary categorization of aggressive white blood cancer is depicted in Figure 7. As shown in Table 2, the CNN has a precision of 95.19% and an accuracy of 97.25%.

$$w(n) = w(n - 1) - \alpha * m(t) / (\sqrt{v(t)} + \epsilon) \quad (5)$$

Where  $w$  represents the weight matrix,  $\alpha$  represents the learning rate;  $m(t)$  and  $v(t)$  represent the bias-corrected estimators of the first and second moments, respectively. The loss curve is shown in Figure 8 for the time spent being trained. The Receiver Operating Characteristic (ROC) graph for the suggested model is depicted in Figure 9. By contrasting the true positive rate (TPR) at varying thresholds with the false positive rate (FPR), we obtain the ROC curve. (FPR). Curves depicting accuracy and memory frequently cross each other and take on a zigzag shape. This complicates the task of comparing two shapes. As a result, we describe an ideal test case as a set of shapes that travel through or are tilted more toward the top right corner. The suggested model has a recall of 0.93 and an accuracy of 1. Figure 10 illustrates the tradeoff between accuracy and memory for each attainable threshold value. As can be seen in Figure 10, our categorization outcomes are very close to the ideal situation of the precision-recall curve.

## B. ANALYSIS USING MACHINE LEARNING

In the following part, we present the results of our comparison study, which demonstrate that deep learning's performance improves with increasing data size. Differencing Machines offers a number of picture categorization methods that we have used to evaluate the suggested deep learning method. In order to use any of the machine learning methods, it is necessary to first take two characteristics from the images: the histogram and the Discrete Fourier Transform (DFT). After this, all models are learned using these characteristics as input. The categorization model was constructed using the 'RBF' kernel by the supervised learning method SVM [31]. For both kinds of cancer, the Gaussian distribution is used by Naive Bayes, a probability predictor [32]. The goal of the decision tree classification model [33] is to make predictions about the value of a variable using the acquired feature vector as input. Random forests are an ensemble learning method that calculates a final score by averaging the predictions of many separate, previously constructed decision trees [34].



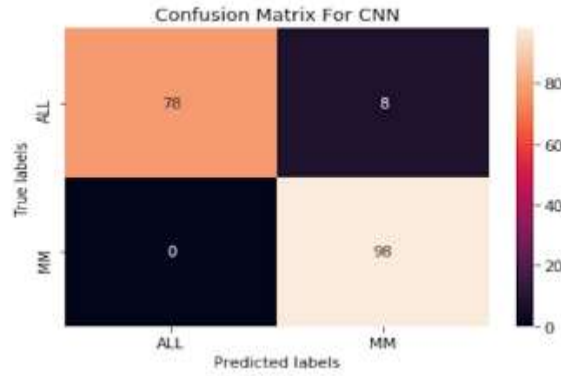


Figure 7: Proposed DCNN Model Confusion Matrix

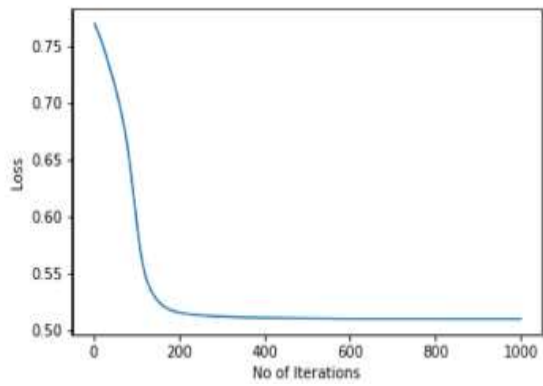


FIGURE 8: Loss vs. Training Iterations Scatter plot

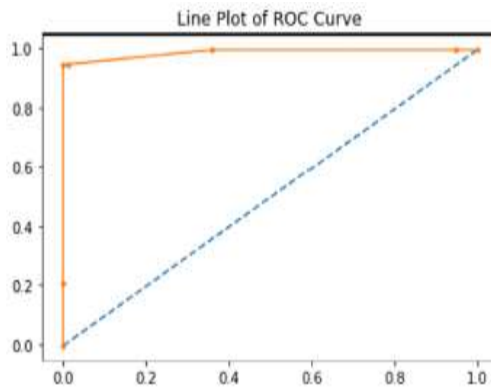


FIGURE 9: ROC Curve for proposed CNN model

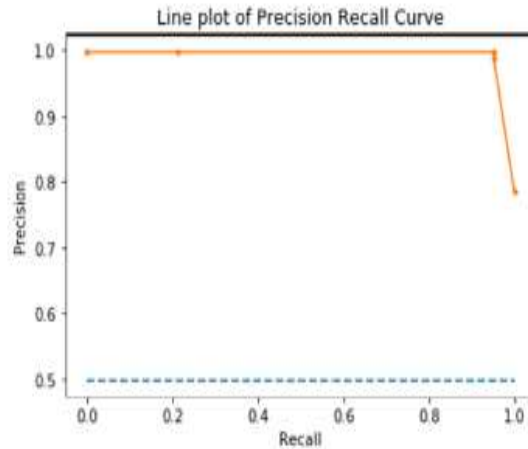


FIGURE 10: Precision-Recall for proposed CNN model

### C. ANALYSIS USING TRANSFER LEARNING

In this work, we demonstrate that the suggested model outperforms VGG-16 and other transferred learning models in order to reduce the computational expense of solving comparable issues. VGG-16 is a simplified example of a convolutional neural network with just three layers. The model consists of two 4096-node completely linked layers, with softmax used for categorization [35]. All of these metrics—Accuracy, Precision, Recall, Specificity, and the F1 Score—have been compared. TP is the proportion of samples that were properly assigned to the positive group. However; TN is the proportion of samples that were properly assigned to the negative class. Samples where the model wrongly forecasts the negative class (FP) and samples where the model incorrectly predicts the positive class (FN) are called false positives and false negatives, respectively. Using Figure 12, we can see that Table 2 is shown.

$$AC = (TP + TN) / (TP + TN + FP + FN) \quad (6)$$

$$P = TP / (TP + FP) \quad (7)$$

$$R = TP / (TP + FN) \quad (8)$$

$$S = TN / (TN + FP) \quad (9)$$

$$F = (2 * P * R) / (P + R) \quad (10)$$

The outcomes of using various machine learning algorithms are displayed in Table 2.

The SVM confusion vectors are depicted in Figure 11. Images can be classified into two groups using Naive Bayes, Decision Trees, and Random Forests. True positives (TP), false positives (FP), true negatives (TN), and false negatives (FN) are the four categories represented in a confusion matrix. (FN). In our system, pictures of ANY type of cancer cell are considered positive, while those of MM cancer cells are considered negative. With an impressive precision of 96.83%, Random Forests has successfully categorized both MM and ALL pictures. Very little preprocessing of the data is required, and it works well with binary or category characteristics.

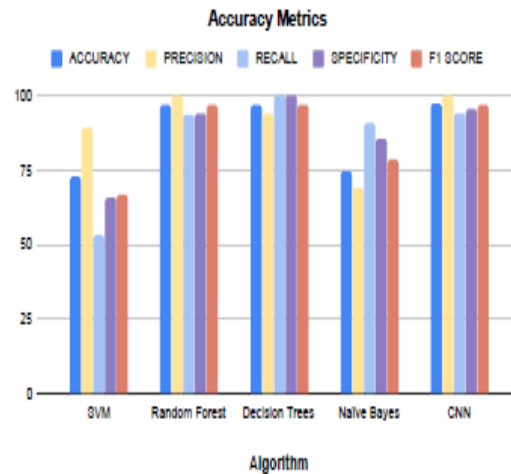


FIGURE 12: Accuracy of the suggested CNN algorithm in terms of recall

Table 3 displays the results of a comparison study of the suggested model applied to various datasets. The first collection of statistics is collected from fertilizing wasps [36]. The information was compiled from footage shot in June 2017 at a bee colony's entryway. The suggested algorithm successfully separated fertilizing pollinators from the rest of the population 82% of the time. Hematoxylin and eosin (H&E) stained slides of blood cancer cells is the next group [37]. There are 116 standardized damaged pictures in the collection. The precision of the suggested algorithm in distinguishing between normal and cancerous data sets is 87%. Finally, 84,495 X-Ray pictures from a collection of retinal OCT images are used for comparison [38]. The suggested algorithm successfully distinguished between infectious and uninfected retinal pictures with an accuracy of 87%.

## V. CONCLUSION

The suggested model employs a deep learning approach, in particular convolutional neural networks, to eliminate the possibility of human error in the traditional method. This is the prototype, before creating the model with the modified Convolutional neural network architecture; it first pre-forms the images and extracts the most salient features. Ultimately, it can determine what kind of cancer is depicted in a picture. A 97.2% precision rating was given to the program. We also compared our results to those obtained using state-of-the-art techniques such as Support Vector Machines (SVMs), Decision Trees, Random Forests, Naive Bayes, etc. The suggested model outperformed the aforementioned approaches. The model's superior precision is demonstrated over three separate datasets, alongside a contrast to other suggested models. As a result, the model is a useful tool for identifying the specific form of bone marrow cancer. However, we must concede that a more comprehensive practical research taking database capacity into account has not been provided here.

## REFERENCES

- [1] Kai Kessenbrock, Vicki Plaks, and Zena Werb. *Matrix metalloproteinases: regulators of the tumor microenvironment*. *Cell*, 141(1):52–67, 2010.
- [2] Amjad Rehman, Naveed Abbas, Tanzila Saba, Syed Ijaz ur Rahman, Zahid Mehmood, and Hoshang Kolivand. *Classification of acute lymphoblastic leukemia using deep learning*. *Microscopy Research and Technique*, 81(11):1310–1317, 2018.
- [3] Sarmad Shafique and Samabia Tehsin. *Acute lymphoblastic leukemia detection and classification of its subtypes using pretrained deep convolutional neural networks*. *Technology in cancer research & treatment*, 17:1533033818802789, 2018.
- [4] Michael Hallek, P Leif Bergsagel, and Kenneth C Anderson. *Multiple myeloma: increasing evidence for a multistep transformation process*. *Blood, The Journal of the American Society of Hematology*, 91(1):3–21, 1998.

- [5] John G Kelton, Alan R Giles, Peter B Neame, Peter Powers, Nina Hageman, and J Hirsch. Comparison of two direct assays for platelet-associated igg (paigg) in assesement of immune and nonimmune thrombocytopenia. 1980.
- [6] Matthias Perking, Johannes Hofmanninger, Björn Menze, Marc-André Weber, and Georg Langs. Detecting bone lesions in multiple myeloma patients using transfer learning. In *Data Driven Treatment Response Assessment and Preterm, Perinatal, and Paediatric Image Analysis*, pages 22–30. Springer, 2018.
- [7] Ahmedin Jemal, Rebecca Siegel, Elizabeth Ward, Yongping Hao, Jiaquan Xu, and Michael J Thun. *Cancer statistics, 2009. CA: a cancer journal for clinicians*, 59(4):225–249, 2009.
- [8] Ying Liu and Feixiao Long. Acute lymphoblastic leukemia cells image analysis with deep bagging ensemble learning. In *ISBI 2019 CNMC Challenge: Classification in Cancer Cell Imaging*, pages 113–121. Springer, 2019.
- [9] Andriy B Kul'chyns'kyi, Valeriy M Kyjenko, Walery Zukow, and Igor L Popovych. Causal neuron-immune relationships at patients with chronic pyelonephritis and cholecystitis. correlations between parameters eeg, hrv and white blood cell count. *Open Medicine*, 12(1):201–213, 2017.
- [10] Sonaal Kant, Pulkit Kumar, Anubha Gupta, Ritu Gupta, et al. Leukonet: Dct-based cnn architecture for the classification of normal versus leukemic blasts in b-all cancer. *arXiv preprint arXiv:1810.07961*, 2018.